

PACS numbers: 52.50.Jm; 42.65.Re; 42.70.Ce
DOI: 10.1070/QE2012v042n10ABEH014896

Femtosecond laser pulse filamentation under anomalous dispersion in fused silica. Part 2. Experiment and physical interpretation

E.O. Smetanina, V.O. Kompanets, S.V. Chekalin, V.P. Kandidov

Abstract. **We have studied experimentally and analytically the formation of the supercontinuum (SC) spectrum during femtosecond laser pulse filamentation in fused silica under conditions of zero and anomalous group velocity dispersions. It is found that with increasing centre wavelength from 1300 to 2300 nm, the SC spectrum of the anti-Stokes wing narrows, shifting to the blue. It is shown that the anti-Stokes (blue) shift of the SC spectrum increases with the multiphoton order of the medium ionisation by the light field in the filament. It is found that a broad minimum in the SC spectrum, separating the anti-Stokes wing from the centre wavelength, is a result of the interference of radiation from a moving broadband source, stemming from self-phase modulation of the high-intensity light field. The interference factors of the SC spectra obtained for this source, which moves along the emitting region of the filament in a dispersive medium, are in agreement with experimental and numerical results.**

Keywords: *filamentation, supercontinuum generation, conical emission.*

1. Introduction

Supercontinuum (SC) generation due to filamentation in condensed media has been most thoroughly experimentally studied for femtosecond pulses of a Ti:sapphire laser [1–8]. A femtosecond pulse of a parametric amplifier at the centre wavelength $\lambda_0 = 1500$ nm was used in investigations of SC generation when either one [9] or many [10] filaments were formed in fused silica. The authors of these papers, paying attention to the fact that a broad minimum in the SC spectrum is formed in the region of the zero group-velocity dispersion (GVD), do not explain the reasons for the emergence of this broad minimum. In studying filamentation of a femtosecond pulse from a parametric amplifier, tunable in the wavelength range 1100–1600 nm, it is found that in the YAG crystal the cutoff wavelength of the SC spectrum in the anti-Stokes (blue) region is equal to 530 nm, regardless of the pulse wavelength [11]. Formation of a blue peak in the SC spectrum under various focusing conditions in a 2-cm-thick silica sample during filamentation of a 1055-nm laser pulse, which lies in the region of the weak normal GVD, is investigated in [12]. To interpret the formation of a broad minimum between the pump pulse spectrum and the blue peak, Faccio et al. [12] use the phase relation for X-waves.

There are various models that explain the formation of the maximum in the anti-Stokes region of the SC during filamentation of a pulse with a near-IR wavelength. In Ref. [13] the formation of a maximum of the spectral intensity in the region of 670 nm during filamentation of a 1600-nm pulse in fused silica was explained by the formation of a shock wave of the envelope due to the self-steepening of the trailing edge of the pulse under conditions of the frequency asymmetry of the contributions of self-phase modulation and multiphoton ionisation. Earlier, by the example of femtosecond pulse filamentation in water, Kolesik et al. [14] showed that the material dispersion of the medium significantly affects the SC spectrum. Theoretical studies [15, 16] developed the model of three-wave mixing, in which the SC radiation is the result of scattering of the light field incident on the material waves emerging in a medium in the case of nonlinear optical interaction of the intense radiation of the filament. The phase-matching condition obtained in the model determines the angle of divergence of the spectral SC components with the maximal intensity. When a soliton propagates in a waveguide under conditions of anomalous mode dispersion, the peak in the anti-Stokes region of the spectrum (according to the numerical [17] and analytical [18] studies) is formed due to the strong influence of the third-order dispersion, and the detuning is determined by the ratio of the dispersion coefficients of the second and third orders.

However, there is currently no convincing physical interpretation of the formation of a maximum in the visible SC spectrum during filamentation of near-IR femtosecond pulses. Theoretical studies [19, 20], based on the results of numerical studies of filamentation of pulses at different wavelengths, concluded that the nature of the maximum in the visible SC spectrum is still open to question.

This paper is a logical continuation of the numerical studies [21], and its goal is to obtain a convincing physical explanation of the process of formation of the SC spectrum and, in particular, of an isolated anti-Stokes wing during femtosecond laser pulse filamentation in fused silica. We present the results of experimental studies of the SC spectrum during filamentation of the pulse, tunable in the wavelength range of 1200–2300 nm, and theoretical studies of the influence of various factors on the structure of the spectrum. To analyse the spectra obtained experimentally, we use the results of numerical simulations presented in [21].

E.O. Smetanina, V.P. Kandidov Department of Physics, M.V. Lomonosov Moscow State University, Vorov'evy gory, 119991 Moscow, Russia; e-mail: smetanina@physics.msu.ru, kandidov@physics.msu.ru;
V.O. Kompanets, S.V. Chekalin Institute of Spectroscopy, Russian Academy of Sciences, ul. Fizicheskaya 5, 142190 Troitsk, Moscow region, Russia; e-mail: kompanetsvo@isan.troitsk.ru, chekalin@isan.troitsk.ru

Received 14 May 2012; revision received 12 July 2012
Kvantovaya Elektronika **42** (10) 920–924 (2012)
Translated by I.A. Ulitkin

2. Experiment

In a laboratory experiment, the source of femtosecond pulses was a TOPAS tunable parametric amplifier combined with a Spitfire Pro regenerative amplifier. The duration of femtosecond radiation was measured with an ASF-20 autocorrelator (Avesta Project). Femtosecond laser pulses were focused by a thin quartz lens with a focal length of 50 cm at the front face of the fused silica sample (Fig. 1). The sample was in the form of an acute-angled wedge, which allows us to vary the length of the filament at specified pulse parameters [22]. The beam diameter at the waist was about 100 μm. The SC radiation was collected by an achromatic lens on the monochromator. A scattering plate mounted on its input window produced scattered radiation, which made it possible to eliminate the influence of the angular dependence of the spectral SC components, which is characteristic of the conical emission. The SC spectrum in the band 400–1000 nm was measured with a Solar-Tii MS2004 monochromator, whereas the SC spectrum in the band 1100–2700 nm was measured with an ASP-IRHS spectrometer, developed by 'Avesta Project' in 2010. The dynamic range of the spectrometers was 10^3.

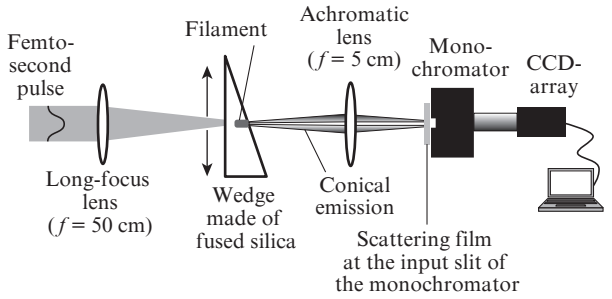

Figure 1. Schematic of the experimental setup.

In the experiments, we used near-IR radiation with a centre wavelength tunable from λ_0 = 1300 nm, corresponding to a zero GVD, to λ_0 = 2300 nm, corresponding to a strong anomalous GVD in fused silica. The FWHM pulse duration was 70 fs. With tuning the wavelength, the radiation energy increased from 2.6 μJ at λ_0 = 1300 nm to 4.5 μJ for λ_0 = 1900 nm, so that the ratio of the peak power P to the critical self-focusing power P_{cr} in fused silica was the same, close to 5. It was assumed that the power P_{cr} was equal to 4.95 MW at a wavelength λ_0 = 1300 nm and increased in accordance with the dependence $P_{cr} \sim \lambda_0^2$. At a wavelength exceeding 2000 nm, the pulse energy had to be increased to 8–12 μJ by increasing absorption in fused silica. In the measurements, the wedge-shaped sample of fused silica was moved in the direction perpendicular to the beam so that to obtain plasma channels of equal length for pulses with different wavelengths. The plasma channels were recorded through the side face of the sample. Since the plasma channel coincides with the region of existence of a high-intensity light bullet, its position and length completely determine the filament region characterised by self-phase modulation of the light field, which causes the broadening of the frequency spectrum of the pulse [21]. By displacing the sample we established an equal length of the emitting regions of the filament for pulses with different wavelengths. In our experiments, the emitting regions of the filament had a length of about 1 mm and were located, for example, at a distance of $\sim$ 8 mm for the pulses with λ_0 = 1300 nm and at a distance of 6.5 mm for the pulses with λ_0 = 1900 nm. Thus, we carried out the registration of the SC spectrum $S_{exp}(\lambda)$, which is formed by the emitting region of equal length in the absence of refocusing during filamentation of pulses with the centre wavelength tunable over a wide range.

Figure 2 presents the experimentally obtained spectra $S_{exp}(\lambda)$ for the three wavelengths λ_0 and the computed spectra $S_{comp}(\lambda)$, discussed in detail in [21]. For each wavelength λ_0 the experimental spectra in the IR region $S_{exp}^{IR}(\lambda)$ (1100 nm $< \lambda <$ 2700 nm) are normalised to the maximum values of $S_{exp}^{IR}(\lambda_0)$. In the visible region (400 nm $< \lambda <$ 1100 nm) the normalisation of the spectra $S_{exp}^{vis}(\lambda)/S_0$ is such that their maximum values are equal to the maximum values of the spectra $S_{comp}(\lambda)$ in this spectral band. The CCD array sensitivity spectral bands of the Solar-Tii MS2004 monochromator for short-wavelength range 400–1200 nm and of the ASP-IRHS spectrometer for IR range 1100–2700 nm are shown in Fig. 2 in bold lines on the wavelength axis.

For pulses at all the wavelengths λ_0 considered, the experimentally obtained spectra $S_{exp}^{vis}(\lambda)$ and $S_{exp}^{IR}(\lambda)$ within the dynamic range of the spectrometer are close to the computed spectra $S_{comp}(\lambda)$. This confirms the conclusion of the existence of the anti-Stokes wing of the SC during filamentation of the femtosecond laser pulse at a wavelength lying in the region of the anomalous GVD. As the centre wavelength λ_0 increases from 1300 to 2100 nm, the SC spectrum becomes essentially nonmonotonic and an anti-Stokes wing is formed as an isolated maximum in the visible wavelength region (Fig. 2). In this case, the spectral width of the Stokes wing narrows down, and the intensity of the spectral components increases, reaching $e^{-5}S(\lambda_0)$. The wavelength of the short-wavelength cutoff of the blue components of the spectrum λ_{min} decreases and the blue shift increases with increasing multiphoton order K of the laser plasma generation process. Narrowing of the width of the anti-Stokes wing and its shift to the blue region of the spectrum with increasing centre wavelength λ_0 were also observed in the experimental photographs of the conical emission of the SC.

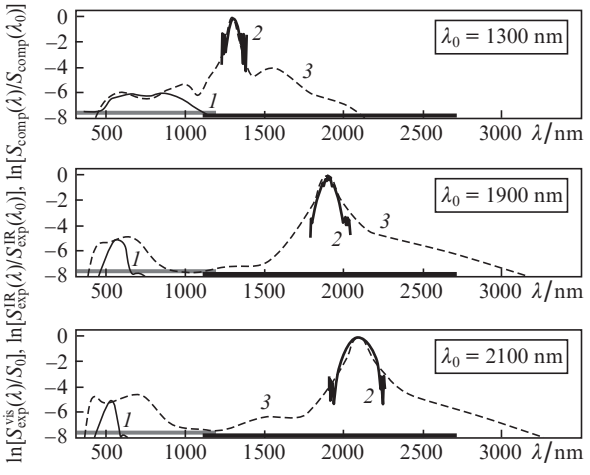

Figure 2. Spectra $S_{exp}^{vis}(\lambda)$ (*1*), $S_{exp}^{IR}(\lambda)$ (*2*) и $S_{comp}(\lambda)$ (*3*) during femtosecond laser pulse filamentation in fused silica under conditions of the zero (λ_0 = 1300 nm, pulse energy 2.6 μJ) and anomalous (λ_0 = 1900 and 2100 nm, pulse energy 4.5 and 8.7 μJ, respectively) GVD. The FWHM pulse duration is 70 fs and the peak power-to-critical self-focusing power is $P/P_{cr} \approx 5$.

3. Influence of multiphoton ionisation and GVD on the SC spectrum

Changing the wavelength λ_0 has a multifactorial influence on the SC spectrum in the case of filamentation. Thus, with increasing λ_0, the multiphoton order $K = [U_i/(\hbar\omega_0) + 1]$ (U_i is the band gap, and ω_0 is the centre frequency of radiation) increases, simultaneously changing the character of the GVD.

In a laboratory experiment with specific media, it is impossible to study separately the effect of each of these factors on the formation of the anti-Stokes wing in the SC spectrum, while a numerical simulation allows for such a study, by considering model media with hypothetical parameters. Let the data on the medium differ from fused silica only by the band gap U_i, and therefore, by the multiphoton order K of the laser plasma generation process. We assume that in medium 1 for radiation at $\lambda_0 = 1900$ nm, the GVD is anomalous as in fused silica, and the multiphoton order is two times smaller. The study of filamentation in this medium will enable us to specify the influence of only the multiphoton order on the SC spectrum at an invariable GVD. For radiation with $\lambda_0 = 1900$ nm Fig. 3 shows the profiles of the pulse on the axis $I(r=0,t)$ and its spectra $S_{comp}(\lambda)$ obtained in the numerical experiment for fused silica with $K = 14$ and for a hypothetical medium 1 with $K_1 = 7$. The results are obtained for the case of one emitting region in the filament. In this case, the duration, energy and peak intensity of the incident light and the propagation distance ($z = 7$ mm) for both media are the same. It is seen that with decreasing multiphoton order K in the medium with the anomalous GVD, the pulse shape $I(r=0,t)$ and pulse spectrum $S_{comp}(\lambda)$ change significantly. With a decrease in K, the rate of the electron density rise in the laser plasma, which causes the defocusing of the pulse tail, is also reduced, and, as a result, the self-steepening of the trailing edge of the pulse is markedly decreased. As a result, self-phase modulation in a medium with a smaller band gap decreases the blue frequency shift in the SC spectrum. In the hypothetical medium 1 with $U_{i1} = 4.5$ eV the anti-Stokes shift $\Delta\omega_{as1}$ is less than the shift in fused silica $\Delta\omega_{as}$, and the ratio $\Delta\omega_{as}/\Delta\omega_{as1} \propto K/K_1$.

For the case of the normal GVD, consider medium 2, in which for the pulse with $\lambda_0 = 800$ nm, the dispersion is the same as in the silica, and the band gap U_{i2} is twice larger. For radiation with $\lambda_0 = 800$ nm Fig. 4 shows the profiles of the pulse on the axis $I(r = 0, t)$ and its spectra $S_{comp}(\lambda)$ obtained at the same distance from the entrance to the medium ($z = 9.1$ mm) for fused silica with $U_i = 9$ eV and $K = 6$, and for a hypothetical medium 2 with $U_{i2} = 20$ eV and $K_2 = 13$. The duration, energy and the peak intensity of the incident light for both media are the same. One can see that in a medium with the normal GVD, the pulse splits, as usual, into subpulses with increasing multiphoton order K (Fig. 4). However, when K is larger, trailing edge of the second subpulse becomes steeper, which entails an increase in the anti-Stokes shift $\Delta\omega_{as}$, so that the ratio $\Delta\omega_{as}/\Delta\omega_{as2} \propto K/K_2$. With increasing SC band, its spectrum exhibits a minimum separating the anti-Stokes wing from the centre wavelength of the pulse.

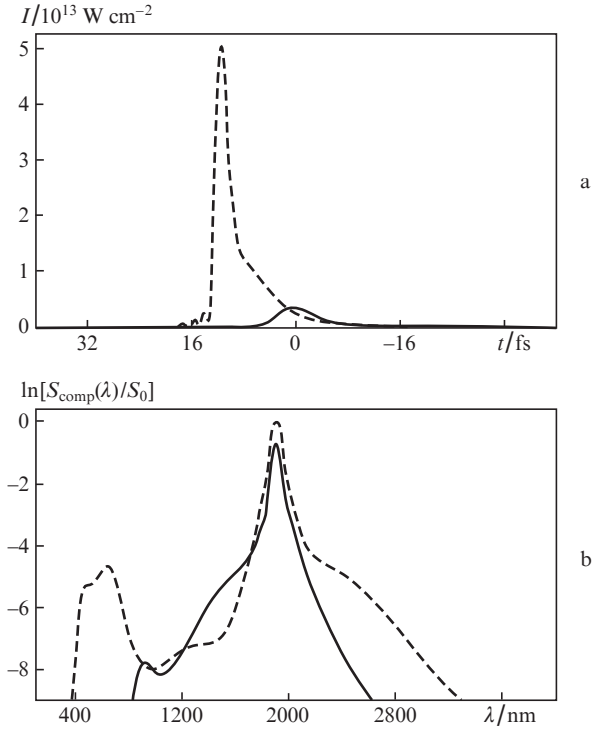

Figure 3. Influence of the band gap under conditions of the anomalous GVD of the medium on the shape $I(r=0,t)$ (a) and spectrum $S_{comp}(\lambda)$ (b) of the pulse at $\lambda_0 = 1900$ nm. Dashed curves are fused silica (band gap $U_i = 9$ eV, multiphoton order $K = 14$), solid curves are a hypothetical medium 1 ($U_{i1} = 4.5$ eV, $K_1 = 7$). The radiation parameters are as follows: peak intensity, $I_0 = 0.268\times10^{12}$ W cm^{-2}; pulse duration, 80 fs at the intensity level e^{-1}; energy, 4 μJ; peak power-to-critical power, $P/P_{cr} = 5$; and propagation distance, $l = 0.7$ cm.

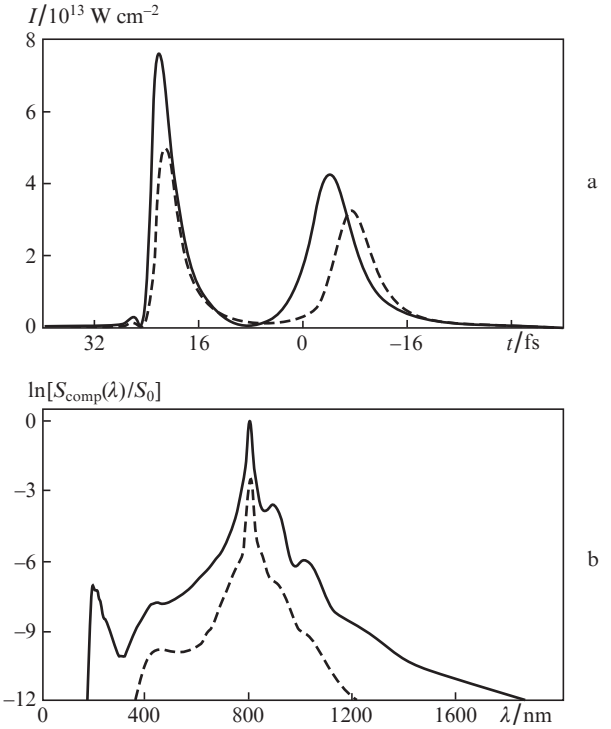

Figure 4. Influence of the band gap under conditions of the normal GVD of the medium on the shape $I(r=0,t)$ (a) and spectrum $S_{comp}(\lambda)$ (b) of the pulse at $\lambda_0 = 800$ nm. Dashed curves are fused silica (band gap $U_i = 9$ eV, multiphoton order $K = 6$), solid curves are a hypothetical medium 2 ($U_{i2} = 20$ eV, $K_2 = 13$). The radiation parameters are as follows: peak intensity, $I_0 = 0.113\times10^{12}$ W cm^{-2}; pulse duration, 80 fs at the intensity level e^{-1}; energy, 0.65 μJ; peak power-to-critical power, $P/P_{cr} = 5$; and propagation distance, $l = 0.91$ cm.

Thus, regardless of the GVD behaviour the anti-Stokes shift in the SC spectrum, $\Delta\omega_{as}$, during filamentation is determined by the multiphoton order K of the laser plasma generation process and increases with increasing K. In multiphoton ionisation, which is predominant in the initial stage of plasma generation, the time gradient of the electron concentration, which is associated with the speed of light defocusing at the pulse tail and, therefore, the slope of its trailing edge, increases with increasing K. Self-phase modulation at a larger steepness of the trailing edge causes a strong enrichment of the spectrum with high-frequency harmonics, which results in an increased anti-Stokes shift $\Delta\omega_{as}$. However, neither self-phase modulation, nor plasma generation at different K, nor GVD behaviour does not explain the formation of a broad minimum in the SC spectrum, formed between the anti-Stokes wing and the region in the vicinity of the centre wavelength λ_0.

4. Interference factor

As follows from the analysis of the formation of the SC spectrum, an isolated anti-Stokes wing is formed in the case of the finite length of the emitting region of the filament. Because the SC radiation is coherent [23], the interference of the light field of an extended emitting region affects dramatically the frequency-angular SC spectrum. According to the interference model [24], the expression for the emission spectrum $S_{interf}(\lambda)$ has the form

$$S_{interf}(\lambda) = \frac{1}{4\pi}\int \zeta_0(\theta,\lambda) l^2 \mathrm{sinc}^2\left[\frac{\Delta\varphi(\theta,\lambda)}{2}\right]\mathrm{d}\theta, \qquad (1)$$

where $\zeta(\theta,\lambda)$ is the frequency-angular SC spectrum of a broadband light point source, which moves with a group velocity of the pulse $v_g(\lambda_0)$, forming an emitting region of length l. A phase shift $\Delta\varphi(\theta,\lambda)$ of the SC emission at a wavelength λ, which is emitted by the source at an angle θ, is described by the expression

$$\Delta\varphi(\theta,\lambda) = \frac{2\pi l}{\lambda_0}\left\{\left(1-\frac{\lambda_0}{\lambda}\right)\frac{c_0}{v_g} - \left[1-\frac{\lambda_0 n(\lambda)}{\lambda n_0}\cos\theta\right]n_0\right\}, \qquad (2)$$

where $n_0 = n(\lambda_0)$ is the refractive index at the centre wavelength and c_0 is the speed of light in vacuum. In (2) the material dispersion of the medium is described by the dependences $v_g(\lambda)$ and $n(\lambda)$, which are calculated according to the Sellmeier formula. The spectrum $\zeta_0(\theta,\lambda)$ is due to self-phase modulation of the light field with increasing slope of the trailing edge of the pulse under conditions of the Kerr and plasma nonlinearities and GVD. The condition for the appearance of the interference maximum in the spectrum (1) is similar to the phase-matching condition for three-wave mixing [14]. Under the assumption that the spectrum of a broadband point SC source is uniform [$\zeta_0(\theta,\lambda) = \mathrm{const}$] and is independent of λ_0, one can analytically calculate the interference factor $F_{interf}(\lambda) = S_{interf}(\lambda)|_{\zeta_0(\theta,\lambda)=1}$, which qualitatively reflects the role of interference in the formation of the SC spectrum. Analysis of the transformation of the amplitudes of the SC component in the interference factor $F_{interf}(\lambda)$ with increasing length of the emitting region can give a physical interpretation of the formation of an isolated anti-Stokes wing of the SC spectrum.

Figure 5 shows the change in the interference factor $F_{interf}(\lambda, l)$ for radiation at 1300 and 1900 nm with increasing length l of the emitting region, which is similar to the dependence of the spectrum $S_{comp}(\lambda, z)$ on z, shown in Fig. 2 in [21]. The interference factor for radiation with $\lambda_0 = 1300$ nm acquires modulation, manifested more strongly with increasing length l. For radiation with $\lambda_0 = 1900$ nm at $l \sim 1$ mm an interference minimum is formed, separating the broad global maximum at the centre wavelength λ_0 and narrow anti-Stokes wing – the maximum in the visible region of the SC spectrum. With a further increase in the length of the emitting region, the interference minimum becomes wider, while the narrow maximum in the anti-Stokes region of the spectrum does not change either its width or spectral position, and becomes even more contrast.

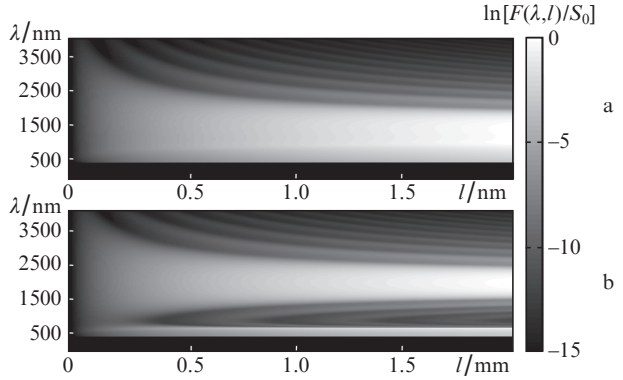

Figure 5. Transformation of the interference factor $F_{interf}(\lambda, l)$ with increasing length of the emitting region, l, for pulses with the centre wavelength $\lambda_0 = 1300$ (a) and 1900 nm (b).

The interference factor $F_{interf}(\lambda_0, \lambda)$, calculated when the centre wavelength λ_0 of the incident radiation changes under the condition of the constant length of the emitting region, l, gives an idea of the impact of interference on the formation of the SC at various GVDs. Figure 6 presents the factor $F_{interf}(\lambda_0, \lambda)$ for the visible region of the spectrum, calculated at $l = 1$ mm, and the spectral map of the SC, $S^{vis}_{exp}(\lambda_0, \lambda)$, obtained experimentally. One can see that for input pulses with $\lambda_0 = 1200$–1500 nm the interference maximum is broad, extending from the centre wavelengths to the visible region of the spectrum (Fig. 6a). With increasing λ_0 the maximum shifts to the blue region of the spectrum with the cutoff wavelength

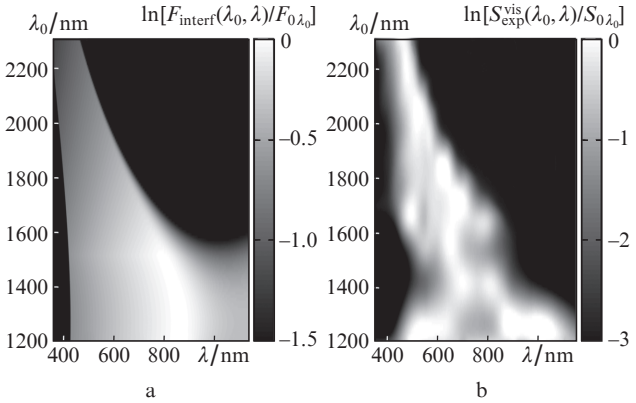

Figure 6. Interference factor $F_{interf}(\lambda_0, \lambda)$ (a) and experimental spectral map $S^{vis}_{exp}(\lambda_0, \lambda)$ of the anti-Stokes wing of the SC (b) for pulses with $\lambda_0 = 1200$–2300 nm at a $\sim$1-mm length of the emitting region of the filament.

of the interference maximum of the anti-Stokes components, and its width decreases. A similar behaviour of the anti-Stokes wing of the SC was observed experimentally in the registration of the spectrum $S^{IR}_{exp}(\lambda_0,\lambda)$ for wavelengths $\lambda_0 = 1200-2300$ nm at the ~1-mm length of the emitting region of the filament (Fig. 6b). As well as the maximum in the anti-Stokes region of the spectrum obtained using the interference factor, the experimentally registered anti-Stokes wing of the SC shifts to the blue with increasing centre wavelength of the input pulse.

Thus, the behaviour of the factor $F_{interf}(\lambda_0)$ calculated from the interference model is qualitatively similar to the behaviour of the spectra $S_{comp}(\lambda)$ and $S^{IR}_{exp}(\lambda_0)$ obtained numerically and experimentally, in spite of the fact that in this model the GVD effect manifests itself only in the phase shift of the spectral SC components with different wavelengths λ. Influence of the multiphoton order of the laser plasma generation process can be taken into account in the interference model by specifying the form and width of the spectrum $\zeta_0(\theta,\lambda)$ of the point source.

5. Conclusions

Regardless of the GVD character, the anti-Stokes shift $\Delta\omega_{as}$ of the SC emission spectrum during filamentation increases with increasing multiphoton order K of the laser plasma generation process. Self-steepening of the trailing edge of the pulse at high K enriches the high-frequency part of the spectrum in the case of self-phase modulation of the light field. In fused silica the high multiphoton order of plasma generation and the associated large anti-Stokes shift of the SC spectrum occur during filamentation of pulses at wavelengths that lie in the region of the anomalous and zero GVD. Therefore, in the case of the anomalous GVD, we observe a significant anti-Stokes shift of the SC spectrum. Formation of a broad minimum in the SC spectrum, separating its anti-Stokes wing from the centre wavelength, during filamentation of femtosecond pulses at wavelengths 1300–2100 nm in fused silica is the result of destructive interference of broadband SC radiation, which is generated in the emitting region of finite length. With an increase in the centre wavelength of radiation under conditions of the anomalous GVD, the width of the anti-Stokes wing of the SC decreases and its shift to the blue region of the spectrum increases.

Acknowledgements. This work was supported by the Russian Foundation for Basic Research (Grant Nos 11-02-00556a and 12-02-31690). Kompanets and Chekalin are grateful for the support of the scientific school headed by Prof. Vinogradov (Grant No. NSh-1049.2012.2). Research of Kandidov and Smetanina was supported by the Grant of the President of the Russian Federation for State Support of Leading Scientific Schools of the Russian Federation (Grant No. NSh-6897.2012.2) and by the grant of the Ministry of Education and Science of the Russian Federation (Grant No. 8393).

References

1. Kandidov V.P., Kosareva O.G., Golubtsov I.S., Liu W., Becker A., Akozbek N., Bowden C.M., Chin S.L. *Appl. Phys. B*, **77**, 149 (2003).
2. Chin S.L., Hosseini S.A., Liu W., Luo Q., Theberge F., Akozbek N., Becker A., Kandidov V., Kosareva O., Schroeder H. *Can. J. Phys.*, **83**, 863 (2005).
3. Couairon A., Mysyrowicz A. *Phys. Rep.*, **441**, 47 (2007).
4. Kandidov V.P., Shlenov S.A., Kosareva O.G. *Kvantovaya Elektron.*, **39**, 205 (2009) [*Quantum Electron.*, **39**, 205 (2009)].
5. Liu W., Petit S., Becker A., Akozbek N., Bowden C.M., Chin S.L. *Opt. Commun.*, **202**, 189 (2002).
6. Nguyen N.T., Saliminia A., Liu W., Chin S.L., Vallée R. *Opt. Lett.*, **28**, 1591 (2006).
7. Dharmadhikari A.K., Rajgara F.A., Mathur D. *Appl. Phys. B*, **82**, 575 (2006).
8. Dachraoui H., Oberer C., Michelswirth M., Heinzmann U. *Phys. Rev. A*, **82**, 043820 (2010).
9. Saliminia A., Chin S.L., Vallée R. *Opt. Express*, **13**, 5731 (2005).
10. Naudeau M.L., Law R.J., Luk T.S., Nelson T.R., Cameron S.M. *Opt. Express*, **14**, 6194 (2006).
11. Bradler M., Baum P., Riedle E. *Appl. Phys. B*, **97**, 561 (2009).
12. Faccio D., Averchi A., Lotti A., Kolesik M., Moloney J.V., Couairon A., Di Trapani P. *Phys. Rev. A*, **78**, 033825 (2008).
13. Liu J., Li R., Xu Z. *Phys. Rev A*, **74**, 043801 (2006).
14. Kolesik M., Katona G., Moloney J.V., Wright E.M. *Phys. Rev. Lett.*, **91**, 043905 (2003).
15. Kolesik M., Wright E.M., Moloney J.V. *Phys. Rev. Lett.*, **92**, 253901 (2004).
16. Kolesik M., Wright E.M., Moloney J.V. *Opt. Express*, **13**, 10729 (2005).
17. Wai P.K.A., Menyuk C.R., Lee Y.C., Chen H.H. *Opt. Lett.*, **11**, 464 (1986).
18. Elgin J.N. *Opt. Lett.*, **17**, 1409 (1992).
19. Skupin S., Bergé L. *Physica D*, **220**, 14 (2006).
20. Bergé L., Mauger S., Skupin S. *Phys. Rev. A*, **81**, 013817 (2010).
21. Smetanina E.O., Kompanets V.O., Chekalin S.V., Kandidov V.P. *Kvantovaya Elektron.*, **42**, 913 (2012) [*Quantum Electron.*, **42**, 913 (2012)].
22. Kandidov V.P., Smetanina E.O., Dormidonov A.E., Kompanets V.O., Chekalin S.V. *Zh. Eksp. Teor. Fiz.*, **140**, 484 (2011).
23. Chin S.L., Brodeur A., Petit S., Kosareva O.G., Kandidov V.P., *J. Nonlinear Opt. Phys. Mater.*, **8**, 121 (1999).
24. Dormidonov A.E., Kandidov V.P. *Laser Phys.*, **19**, 1993 (2009).